© Universiti Tun Hussein Onn Malaysia Publisher's Office

IJIE

Journal homepage: http://penerbit.uthm.edu.my/ojs/index.php/ijie
ISSN : 2229-838X e-ISSN : 2600-7916

The International Journal of Integrated Engineering

Analysis of Soil Liquefaction Potential through Three Field Tests-Based Methods: A Case Study of Babol City

Ali Hasanzadeh[1*], Sadegh Rezaei[1,2], Issa Shooshpasha[1], Yasser Ebrahimian Ghajary[1]

[1]Department of Civil Engineering,
Babol Noshirvani University of Technology, Babol, Mazandaran, IRAN

[2]Department of Engineering,
Shargh-e Golestan Institute of Higher Education, Gonbad Kavus, Golestan, IRAN

*Corresponding Author

DOI: https://doi.org/10.30880/ijie.2021.13.04.027
Received 21 May 2020; Accepted 18 April 2021; Available online 02 May 2021

Abstract: During earthquakes, ground failure is commonly caused by liquefaction. Thus, assessment of soil liquefaction potential in earthquake-prone regions is a crucial step towards reducing earthquake hazard. Since Babol city in Iran country is located in a high seismic area, estimation of soil liquefaction potential is of great importance in this city. For this purpose, in the present research, using field-based methods and geotechnical data (such as unit weight of soil, relative density, SPT number, shear wave velocity and cone tip resistance) of 60 available boreholes in Babol, three liquefaction maps were provided. Finally, one comprehensive liquefaction map was presented for soil of Babol city. The obtained results in this paper are well in line with the previous investigations. Based on the results, the factor of safety in 45% of the study area is less than one (liquefaction occurrence). In addition, the results indicate that since each field-based method requires particular data, applying various field tests is necessary for a more accurate liquefaction assessment.

Keywords: Liquefaction, Andrus & Stokoe method, Boulanger & Idriss method, Moss et al. method, liquefaction map

1. Introduction

Landslide and particularly liquefaction have been responsible for extensive damages to infrastructures and residential lands in recent earthquakes around the world [1]-[4]. Liquefaction phenomenon is associated with the development of large pore-water pressures in soils due to cyclic loading effects of earthquakes. Consequently, effective stress reduces and soil loses its strength. The investigation of failure of soil masses during earthquakes requires sciences of geology and engineering [5], [6]. To confront destructive effects of liquefaction, the assessment of soil liquefaction potential and recognition of liquefiable regions are essential. There are several laboratory tests for evaluation of soil liquefaction potential such as cyclic triaxial and cyclic torsional shear tests. Since extracting high quality undisturbed specimens is relatively expensive and the simulation of actual field conditions in laboratory is difficult, approaches based on in-situ tests such as shear wave velocity (Vs) test, Cone Penetration Test (CPT) and Standard Penetration Test (SPT) are widely accepted for estimation of soil liquefaction.

The SPT, due to its simplicity of execution, is one of the most popular in-situ testing techniques used to achieve idea about the stratigraphic profile at a site [7]-[9]. SPT-based approaches have been accepted for evaluation of soil liquefaction and Standard Penetration resistance has been utilized as an index of soil liquefaction resistance during

*Corresponding author: a_hasanzade64@yahoo.com

earthquakes in engineering practice. Development of SPT-based methods began in Japan by studies performed by some investigators such as Kishida [10] and Ohsaki [11]. Then, many researchers studied and recommended procedures for estimation of liquefaction using SPT [12]-[19].

The CPT is an advantageous test in identifying subsurface conditions and estimating different characteristics of soil. Moreover, it is able to provide a continuous record of the penetration resistance. In comparison with SPT, CPT is less vulnerable to operator error and can find thin liquefiable strata that are missed by SPT. However, by CPT, no sample can be obtained. Development of CPT-based methods for evaluation of liquefaction began with work by Zhou [20]. Then, various investigators assessed CPT-based liquefaction methods [21]-[28].

Moreover, applying Vs measurements for assessing the liquefaction resistance of soil is an effective method because Vs and liquefaction resistance are impacted by similar factors (such as state of stress, void ratio and geologic age). Vs can be determined in situ using cross-hole, down-hole and Spectral Analysis of Surface Waves (SASW) tests [29]-[31]. Generally, the SPT and CPT are not useful in gravelly soils due to interference from large-size particles while the measurement of Vs is possible in such soils. In addition, the accuracy of various types of Vs tests is higher than that of penetration tests. However, Vs testing does not produce specimens for classification or may not be performed with adequate details to specify thin liquefiable layers for large measurement intervals. Numerous investigations have been carried out about the liquefaction resistance- Vs relationship [32]-[42]. Although some researchers conducted studies about soil liquefaction potential of Babol city [43]-[45], the obtained results were different because they applied only limited field database in their investigations. Considering that many factors such as soil type, fines content, type of test and its precision can affect liquefaction evaluation, it would be much safer to conduct different field tests for the same place and then compare the results. Therefore, to fill the aforementioned gap in the assessment of soil liquefaction potential of Babol city, three different analysis methods considering various data were selected in this paper: (i) Boulanger & Idriss [46] method (which is a SPT-based method), (ii) Andrus & Stokoe [47] method (which is a Vs-based method), and (iii) Moss et al. [48] method (which is a CPT-based method). In the present research, first, seismology and geology of Babol are introduced. Then, the utilized approaches for estimation of soil liquefaction potential in this city are briefly reviewed. Finally, soil liquefaction potential of Babol city is studied using the mentioned approaches and the obtained results are compared.

2. Seismology and Geology of Babol

The study area in this paper is Babol city, which is located in Mazandaran province in the north of Iran. This city is situated in front of Alborz mountain which is tectonically an active region. Due to the convergent motion between Eurasia and Arabia, which probably began in the Cretaceous period, the tectonic of Alborz Mountain is controlled by boundary conditions [49], [50]. The area around Babol has suffered various earthquakes over the years. The first historically reported great earthquake in this region was Amol earthquake that took place in 1809. This earthquake was felt in a very large district and damaged Babol city [5]. Chahar Dange earthquake destroyed many villages in 1935. Band Pey earthquake killed 1600 people and razed many structures to the ground with over 25 million dollars economical toll in 1957 [51]. Recently, Babol was influenced by the occurrence of the moderate shaking at Kojoor and Marzi Kola earthquakes. Table 1 shows the locations, sources, years of occurrence, intensities and magnitudes of great earthquakes occurred in and around Babol. Babol region consists of soft deposits and is situated in a high seismic zone. In addition, this city lies on the eastern side of Babolrood river and receives abundant rainfall annually. Therefore, the assessment of liquefaction potential in this area is very important. Figure 1 depicts the distribution of groundwater level in Babol city according to the underground water level data collection in the geotechnical boreholes. According to the geolithological variations, the subsurface soil column at Babol city can be categorized into five groups: (i) Extremely loose to medium sand deposits from the surface to 15 m depth with a groundwater table (G.W.T.) less than 1 m, (ii) Thin top layer of silt (3-5 m with SPT-N= 15-20) underlain by thick layer of loose fine sand with some gravel (10-15 m with SPT-N= 10-20) below the ground level. It should be remarked that SPT-N is Standard Penetration Test number, (iii) Thick top layer of clay (8-15 m with SPT-N = 10-15) underlain by thin layer of loose fine sand with some gravel (3-6 m with SPT-N = 15-20) below the ground level, (iv) Thick layer of clay (20-30 m with SPT-N = 20-25), and (v) Thick layer of sand (15-20 m with SPT-N = 15-25). Fig. 2 shows classification of the subsurface soil at Babol city.

Table 1 - List of large earthquakes around and in Babol [5]

Location	Source	Year	Magnitude	Intensity	Liquefaction occurrence
Amol	20 km west of Babol	1809	6.5	IX	Yes (due to great magnitude)
Talar Rood	35 km southeast of Babol	1935	5.7	VII	No
Chahar Dange	60 km southeast of Babol	1935	6.3	VIII	Yes (due to site effect)
Band Pey	10 km west of Babol	1957	6.8	IX	Yes (due to great magnitude)
Babol	Babol	1971	5.2	VI	No
Kojoor	60 km northwest of Babol	2004	6.3	VIII	Yes (due to near field earthquake)
Marzi Kola	Babol	2012	5	VI	No

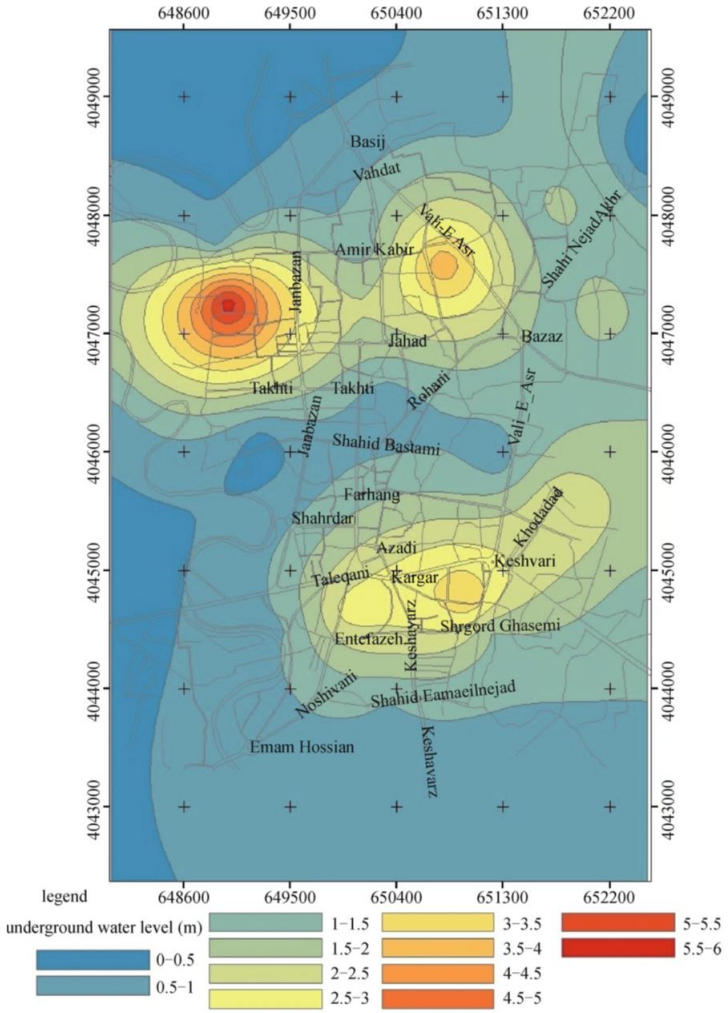

Fig. 1 - The distribution of groundwater level in Babol (typical and not to scale)

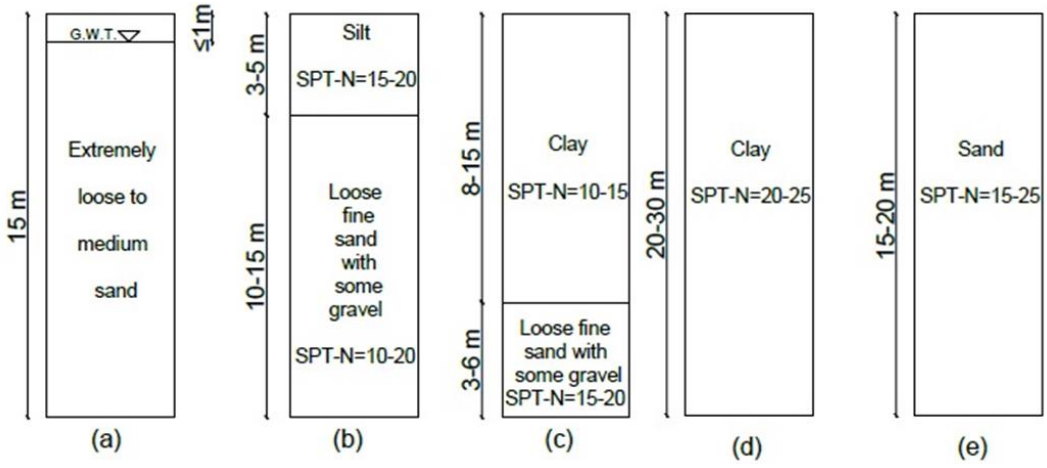

Fig. 2 - Classification of the subsurface soil at Babol city

3. Liquefaction Analysis Approaches

Boulanger & Idriss [46] investigated the liquefaction potential of soil during various earthquakes using SPT and suggested some relations for engineering applications. Andrus & Stokoe [47] presented an approach for the estimation of liquefaction potential through measurement of Vs. Their method was focused on field performance data from 26 earthquakes and measurements of the in-situ Vs at over 70 locations. Moss et al. [48] evaluated the probability of liquefaction using CPT and proposed a correlation for CPT-based estimation of seismically induced liquefaction.

3.1 Boulanger & Idriss Method

Boulanger & Idriss [46] utilized the Seed and Idriss [52] simplified procedure to assess the cyclic stress ratio (CSR) caused by earthquake ground motions:

$$CSR = 0.65\left(\frac{\sigma_{vo}}{\sigma_{vo}^{'}}\right) r_d a_{max} \quad (1)$$

in which a_{max} is the peak horizontal ground surface acceleration (as a fraction of gravity), r_d is the shear stress reduction coefficient and σ_{vo} and $\sigma_{vo}^{'}$ are the total and effective vertical stress at depth z (m), respectively. The r_d is expressed as:

$$Ln(r_d) = \alpha(z) + \beta(z)M \quad (2)$$

$$\alpha(z) = -1.012 - 1.126\,Sin\left(\frac{z}{11.73} + 5.133\right) \quad (2a)$$

$$\beta(z) = 0.106 + 0.118\,Sin\left(\frac{z}{11.28} + 5.142\right) \quad (2b)$$

where M is moment earthquake magnitude. These equations are regarded suitable for $z \leq 34$ m. For $z > 34$ m, Eqn. (2c) is applicable:

$$r_d = 0.12\exp(0.22M) \quad (2c)$$

Magnitude scaling factor (MSF) is utilized to account for shaking duration or equivalent number of stress cycles:

$$MSF = 6.9\exp\left(\frac{-M}{4}\right) - 0.058 \leq 1.8 \quad (3)$$

Overburden correction factor for cyclic stress ratio (K_σ) is determined by the following relation:

$$K_\sigma = 1 - C_\sigma \ln\left(\frac{\sigma'_{vo}}{P_a}\right) \leq 1.0 \quad (4)$$

in which P_a is the reference stress of 101 kPa or approximately atmospheric pressure. The coefficient C_σ is obtained by:

$$C_\sigma = \frac{1}{18.9 - 2.55\sqrt{(N_1)_{60}}} \leq 0.3 \quad (4a)$$

where $(N_1)_{60}$ is the modified SPT number and its maximum value is limited to 37. $(N_1)_{60}$ is adjusted to an equivalent clean sand value ($(N_1)_{60cs}$) as:

$$(N_1)_{60cs} = (N_1)_{60} + \Delta(N_1)_{60} \quad (5)$$

$$\Delta(N_1)_{60} = \exp\left(1.63 + \frac{9.7}{FC + 0.01} - \left(\frac{15.7}{FC + 0.01}\right)^2\right) \quad (5a)$$

where FC is fines content. The cyclic resistance ratio (CRR) can be expressed as:

$$CRR = \exp\left\{\frac{(N_1)_{60cs}}{14.1} + \left(\frac{(N_1)_{60cs}}{126}\right)^2 - \left(\frac{(N_1)_{60cs}}{23.6}\right)^3 + \left(\frac{(N_1)_{60cs}}{25.4}\right)^4 - 2.8\right\} \quad (6)$$

The factor of safety (FS) in this method is found by:

$$FS = \frac{CRR}{CSR} \times MSF \times K_\sigma \quad (7)$$

Liquefaction is predicted to take place for $FS \leq 1$ (i.e., the loading exceeds the resistance).

3.2 Andrus & Stokoe Method

Andrus & Stokoe [46] used Eqn. (1) and Eqn. (2) for determination of CSR and parameter r_d, respectively. They suggested the following relation for determination of CRR:

$$CRR = \left\{ a\left(\frac{V_{s1}}{100}\right)^2 + b\left(\frac{1}{V_{s1}^* - V_{s1}} - \frac{1}{V_{s1}^*}\right)\right\} MSF \tag{8}$$

in which V_{s1} and V^*_{s1} are the overburden stress-corrected V_s and the limiting upper value of V_{s1} for cyclic liquefaction occurrence, respectively. Parameters a and b are the parameters of curve fitting taken to be 0.022 and 2.8, respectively and MSF is calculated by Eqn. (3). V_{s1} is obtained by:

$$V_{s1} = V_s C_V = V_s \left(\frac{P_a}{\sigma'_v}\right)^{0.25} \tag{8a}$$

in which σ'_v, P_a and C_V are the initial effective overburden stress (kPa), atmospheric pressure and overburden stress correction factor, respectively. The maximum C_V value is 1.4 which is usually applied to shear wave velocity data at shallow depths. They expressed the relationship between FC and V^*_{s1} as:

$$V^*_{s1}=215 \text{ m/s for sands with FC} \leq 5\% \tag{8b}$$

$$V^*_{s1}=215-0.5(FC-5) \text{ m/s for sands with } 5\%<FC<35\% \tag{8c}$$

$$V^*_{s1}=200 \text{ m/s for sands with FC} \geq 35\% \tag{8d}$$

It should be mentioned that if $V_{s1} > V^*_{s1}$, no liquefaction is predicted to occur in this method. The FS in this approach can be found by:

$$FS = \frac{CRR}{CSR} \tag{9}$$

when FS ≤ 1, liquefaction happens.

3.3 Moss et al. Method

In Moss et al. [47] method, CSR is obtained using Eqn. (1). The r_d in this method for d < 20 m (d = depth in meters) is defined as:

$$r_d\left(d, M_w, a_{max}\right) = \frac{\left[1+\frac{-9.147-4.173a_{max}+0.652M_w}{10.567+0.089e^{0.089(-3.28d-7.760a_{max}+78.576)}}\right]}{\left[1+\frac{-9.147-4.173a_{max}+0.652M_w}{10.567+0.089e^{0.089(-7.760a_{max}+78.576)}}\right]} \tag{10a}$$

and for d ≥ 20m, parameter of r_d is defined as:

$$r_d\left(d, M_w, a_{max}\right) = \frac{\left[1+\frac{-9.147-4.173a_{max}+0.652M_w}{10.567+0.089e^{0.089(-3.28d-7.760a_{max}+78.567)}}\right]}{\left[1+\frac{-9.147-4.173a_{max}+0.652M_w}{10.567+0.089e^{0.089(-7.760a_{max}+78.567)}}\right]} - 0.0014\left(3.28d-65\right) \tag{10b}$$

in which, M_w is moment magnitude. Magnitude correlated duration weighting factor (DWF_M) is calculated using the following equation:

$$DWF_M = 17.84M_w^{-1.43} \tag{11}$$

In this method, q_{c1} is the normalized tip resistance (MPa):

$$q_{c1} = C_q q_c \tag{12}$$

$$C_q = \left(\frac{P_a}{\sigma'_v}\right)^c \leq 1.7 \tag{12a}$$

in which q_c is raw tip resistance (MPa) obtained by CPT, C_q is tip normalization factor, σ'_v is effective overburden stress (kPa), P_a is atmospheric pressure and c is tip normalization exponent:

$$c = f_1\left(\frac{R_f}{f_3}\right)^{f_2} \tag{12b}$$

$$f_1 = x_1.q_c^{x_2}, x_1 = 0.78, x_2 = -0.33 \quad (12c)$$

$$f_2 = -\left(y_1.q_c^{y2} + y_3\right), y_1 = -0.32, y_2 = -0.35, y_3 = 0.49 \quad (12d)$$

$$f_3 = \text{abs}\left[\log\left(10 + q_c\right)\right]^{z_1}, \qquad z_1 = 1.21 \quad (12e)$$

where R_f is friction ratio in CPT (the ratio of sleeve to tip resistance, in percent). The CRR is found by:

$$\text{CRR} = \exp\left[\frac{q_{c1}^{1.045} + 0.11q_{c1}R_f + 0.001R_f + c\left(1 + 0.85R_f\right) - 0.848\ln\left(M_w\right) - 0.002\ln\left(\sigma'_v\right) - 20.923 + 1.632\phi^{-1}(P_L)}{7.177}\right] \quad (13)$$

in which PL and ϕ^{-1} are the liquefaction probability and the inverse cumulative normal distribution function, respectively. The FS is achieved by:

$$\text{FS} = \frac{\text{CRR}}{\text{CSR}} \times \text{DWF}_M \quad (14)$$

Similar to Boulanger & Idriss [46] and Andrus & Stokoe [47] methods, FS ≤ 1 shows soil liquefaction.

4. Assessment of the Liquefaction Potential in the Study Area

The reliable prediction of liquefaction in any study area is strongly dependent on the quality of the site characterization. Thus, to assess the liquefaction potential of Babol soil through three mentioned approaches, a total number of 60 borehole logs were collected for the present research. Fig. 3 shows the location map of Babol and the location of available geotechnical boreholes in this city. The average distance between the boreholes has been 500m. To determine the shear wave velocity, down-hole tests were performed in boreholes. Moreover, CPT tests were conducted at the nearest possible locations to boreholes. Based on site investigations, the most liquefiable layers were found in some boreholes such as B1 (Fig. 4) in which Vs and q_c show shear wave velocity and cone tip resistance, respectively.

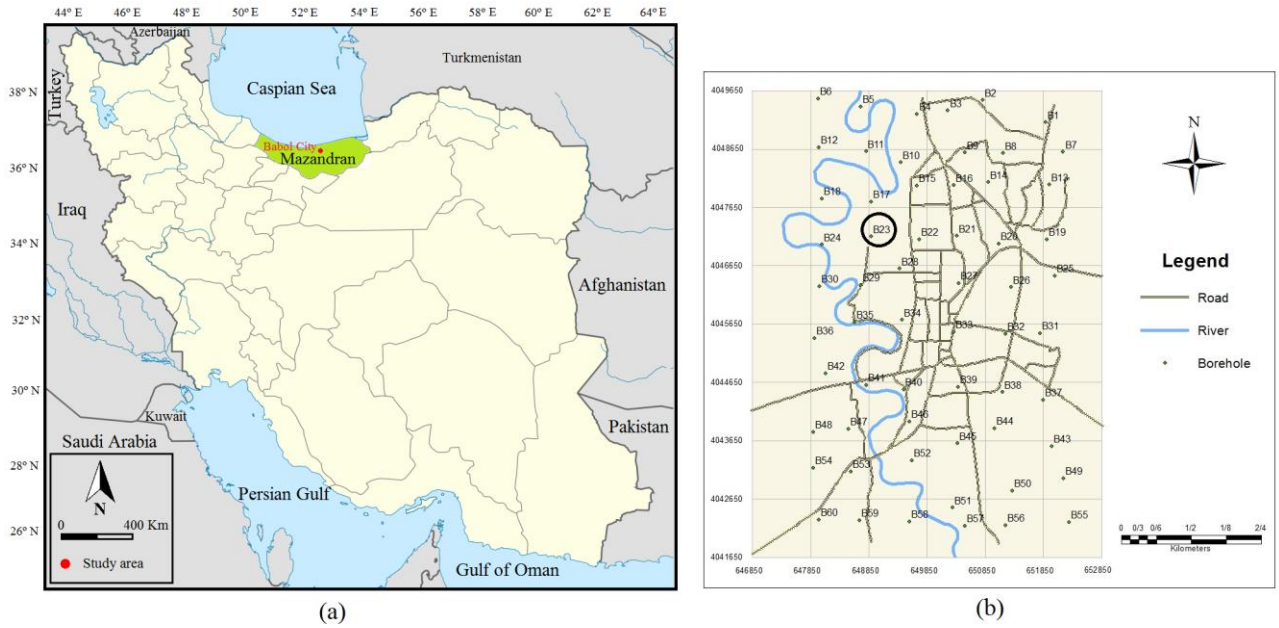

(a) (b)

Fig. 3 - (a) Location map of Babol, and (b) Location of geotechnical boreholes

Since presenting complete results for all boreholes is not possible, one borehole (B23) is selected and the results obtained for this borehole are described completely. The obtained results for other boreholes are presented by liquefaction maps. Fig. 5 and Table 2 show stratigraphy and properties of soil recognized by borehole B23, respectively. In Table 2, w, γ, PI, PL, LL, FC, D_{50}, D_r, N, R_f, V_s and q_c depict water content, unit weight of soil, plasticity index, plastic limit, liquid limit, fine content, mass-median diameter, relative density, SPT number, friction ratio, shear wave velocity and cone tip resistance, respectively. As observed in Fig. 5, the depth of borehole B23 is 20 m and the G.W.T. is 4 m below the ground surface. In addition, PGA (peak ground acceleration) values were selected in each borehole position according to Standard 2800 [53]. At the location of borehole B23, PGA has been 0.35 g (g is

the gravity acceleration). In this research, the M_w is assumed 8. Hence, the calculated MSF and DWF_M values required for liquefaction analysis are 0.87581 and 0.9119, respectively. Table 3 to Table 5 present evaluation of liquefaction potential for borehole B23 using Boulanger & Idriss [46] method, Andrus & Stokoe [47] and Moss et al. [48] methods, respectively. In the analysis of liquefaction, FS at various depths of boreholes are calculated.

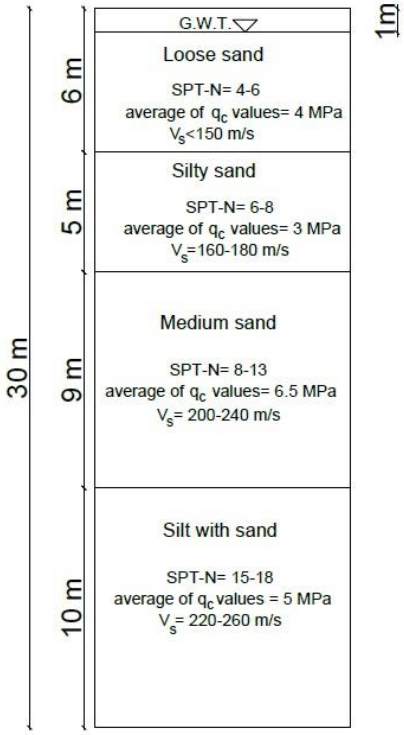

Fig. 4 - Exploratory boring log (borehole B1)

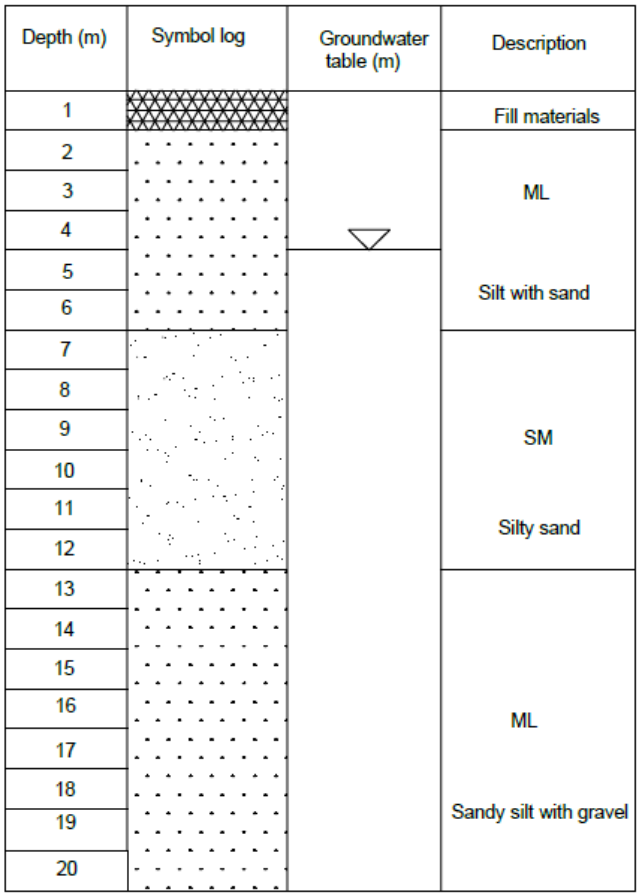

Fig. 5 - Exploratory boring log (borehole B23)

Table 2 - Soil properties (borehole B23)

Depth (m)	w (%)	γ (kN/m³)	LL (%)	PL (%)	PI (%)	FC (%)	D_{50} (mm)	D_r (%)	N	R_f (%)	q_c (MPa)	V_s (m/s)
2	12	17.1	33	27	6	90.5	0.015	52	17	1.60	5.1	210
4	14	17.5	32	25	7	92.8	0.012	59	24	3.50	7.9	230
6	15	17.3	32	25	7	91.5	0.0065	49	19	3.40	7.1	207
8	17	17.2	23	20	3	22.6	1.6	45	25	2.80	9.8	198
10	-	17.3	-	-	-	14.3	2.0	44	22	2.30	8.9	200
12	20	17.3	27	21	6	10.1	2.2	42	27	2.60	10.2	190
14	22	16.5	30	23	7	55.5	0.05	29	15	2.80	7.8	165
16	-	16.8	-	-	-	60.4	0.11	35	21	2.90	9.2	180
18	-	17.6	-	-	-	51.8	0.42	44	29	3.00	11.4	195
20	23	18.1	-	-	-	54.6	0.42	45	34	2.90	14.3	200

Table 3 - Liquefaction analysis using Boulanger & Idriss [46] method for borehole B23

Depth (m)	r_d	CSR	C_σ	K_σ	$(_1N)_{60cs}$	CRR	FS
2	0.99	0.22	0.13	1.00	26.0	0.31	1.23
4	0.98	0.22	0.15	1.00	29.3	0.45	1.79
6	0.96	0.27	0.13	1.00	25.1	0.29	0.94
8	0.95	0.30	0.15	1.00	28.8	0.42	1.22
10	0.93	0.32	0.13	0.98	23.9	0.27	0.72
12	0.91	0.33	0.15	0.96	25.7	0.31	0.78
14	0.88	0.34	0.10	0.97	18.2	0.19	0.47
16	0.86	0.34	0.12	0.95	22.7	0.24	0.58
18	0.84	0.34	0.15	0.92	28.9	0.42	0.99
20	0.81	0.34	0.17	0.89	32.3	0.68	1.55

Table 4 - Liquefaction analysis using Andrus & Stokoe [47] method for borehole B23

Depth (m)	r_d	CSR	V_{s1} (m/s)	V^*_{s1} (m/s)	CRR	FS
2	0.99	0.22	275.29	200	-	No Liquefaction
4	0.98	0.22	252.80	200	-	No Liquefaction
6	0.96	0.27	216.63	171.75	-	No Liquefaction
8	0.95	0.30	198.99	206.2	0.40	1.33
10	0.93	0.32	194.03	210.35	0.21	0.65
12	0.91	0.33	178.72	200	0.16	0.48
14	0.88	0.34	151.42	189.75	0.09	0.26
16	0.86	0.34	161.35	200	0.10	0.29
18	0.84	0.34	170.69	200	0.12	0.35
20	0.81	0.34	171.09	215	0.10	0.29

Table 5 - Liquefaction analysis using Moss et al. [48] method for borehole B23

Depth (m)	r_d	CSR	c	CRR	FS
2	0.95	0.21	0.42	0.30	1.30
4	0.89	0.20	0.28	0.43	1.86
6	0.82	0.23	0.30	0.31	1.23
8	0.74	0.23	0.29	0.45	1.78
10	0.67	0.23	0.32	0.32	1.26
12	0.61	0.22	0.29	0.39	1.61
14	0.58	0.22	0.31	0.24	0.99
16	0.55	0.22	0.29	0.30	1.24
18	0.54	0.22	0.27	0.44	1.82
20	0.52	0.21	0.25	0.68	2.95

Fig. 6 shows the comparison between CRR values determined for borehole B23 using these methods. As seen, CRR values obtained using Boulanger & Idriss [46] and Moss et al. [48] methods show acceptable agreement with each other. However, the obtained CRR values using Andrus & Stokoe [47] method are different. It should be noted that case history data and suggested CRR-V_{S1} curves by Andrus & Stokoe [47] are restricted to relatively level ground sites with a mean depth of less than 10 m. Therefore, for depths more than 10 m, the obtained CRR values of Andrus & Stokoe [47] are different from the ones found using Boulanger & Idriss [46] and Moss et al. [48] approaches. Furthermore, since for depths < 8 m, V_{s1} is higher than V^*_{s1}, no liquefaction is predicted to take place using Andrus & Stokoe [47] method. Fig. 7 shows the comparison between CSR values determined for borehole B23 using these methods. As seen, CSR values obtained using Boulanger & Idriss [46] and Andrus & Stokoe [47] methods are the same. However, CSR values obtained by Moss et al. [48] are less than CSR values obtained by two other methods because the obtained shear stress reduction coefficient (r_d) values in Moss et al. [48] method are less than the values determined using Boulanger & Idriss [46] and Andrus & Stokoe [47] methods. Fig. 8 demonstrates the comparison between FS values for borehole B23 using these methods.

Boulanger & Idriss [46] and Andrus & Stokoe [47] methods have predicted similar results. However, the results predicted by Moss et al. [48] are totally different. In other words, Moss et al. [48] method has predicted that all layers

will be non-liquefiable that can be related to the low CSR and high FS values obtained using this method. Moreover, the results indicate that Andrus & Stokoe-based factor of safety curve is more conservative than factor of safety curves found through Boulanger & Idriss [46] and Moss et al. [48] methods.

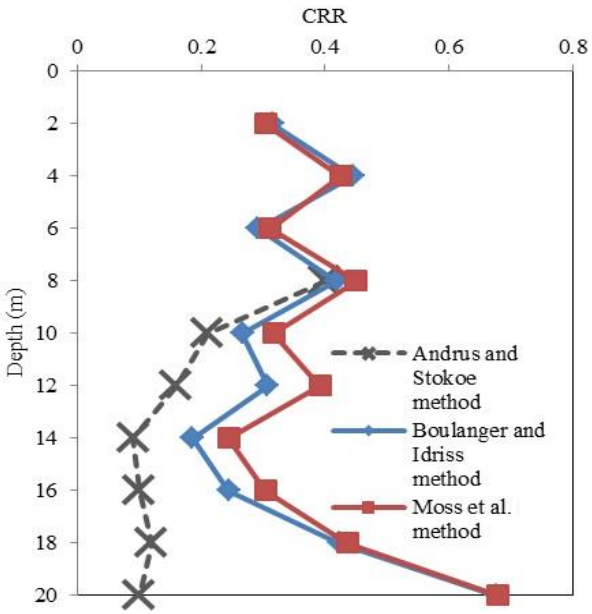

Fig. 6 - Comparison of CRR values for borehole B23

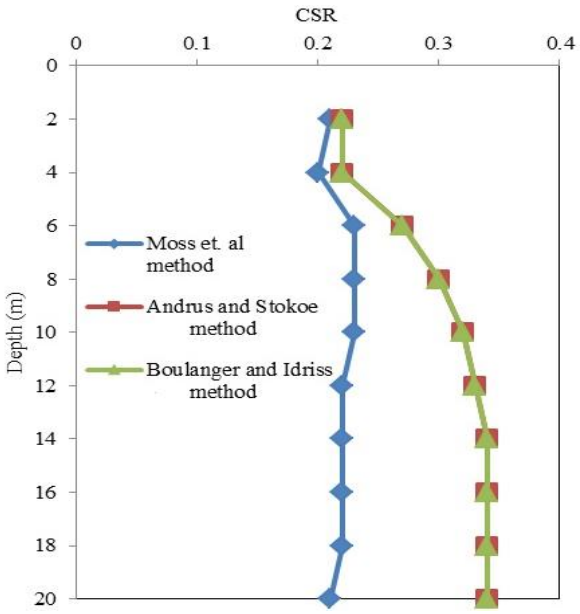

Fig. 7 - Comparison of CSR values for borehole B23

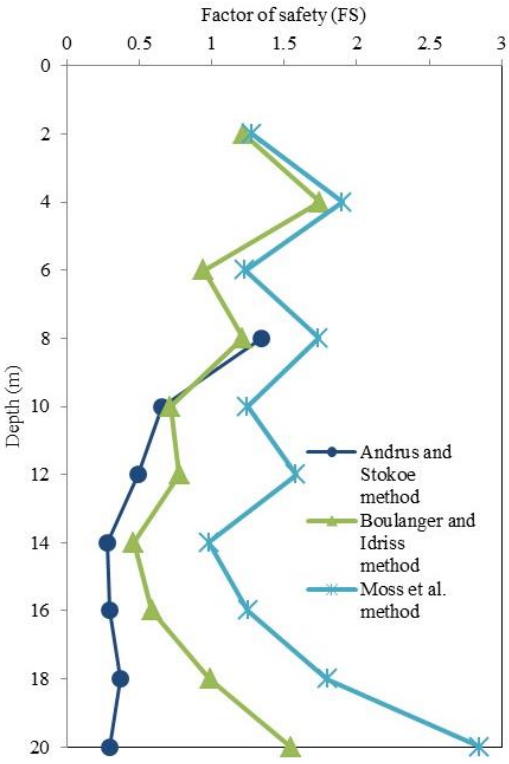

Fig. 8 - Comparison of FS values for borehole B23

For other boreholes, the minimum value of factor of safety in each of them was considered. Figures 9-11 indicate liquefaction maps of Babol using Boulanger & Idriss [46], Andrus & Stokoe [47] and Moss et al. [48] methods, respectively. According to the results, liquefaction occurs in 36, 51 and 31% of boreholes using Boulanger & Idriss [46], Andrus & Stokoe [47] and Moss et al. [48] methods, respectively. Thus, application of Andrus & Stokoe [47] method is conservative. Moreover, using Moss et al. [48] method has high risk in evaluation of liquefaction potential in this city. One of the reasons for the similarity of the results using CPT- and SPT-based approaches is related to the key

role of relative density in estimation of liquefaction [54]. However, since V_s-based methods are less dependent on relative density, the obtained results using Andrus & Stokoe [47] method were different. Figure 12 shows the average of the results obtained by these three methods. The average results indicate that liquefaction (factor of safety of less than 1) occurs in 45% of the boreholes in Babol city. In addition, in 26, 8, 10 and 11% of the boreholes, factor of safety is between 1 and 1.25, 1.25 and 1.5, 1.5 and 2, 2 and 2.5, respectively. It should be noted that Figures 9-12 were drawn using ArcGIS software. Liquefaction map incorporates seismologic, geotechnical and geologic concerns into sociologically and economically land-use planning for earthquake effects and can present useful information to the engineers for the seismic structural design. In addition, engineers can decide about the types of new structures that are most appropriate to be constructed in a specific region using liquefaction map.

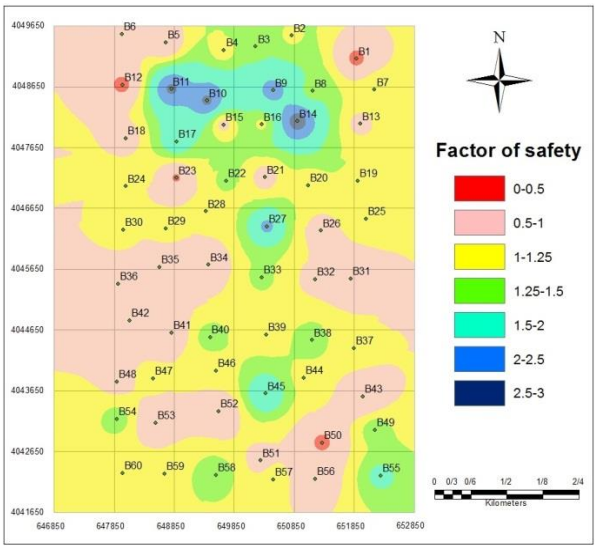

Fig. 9 - Liquefaction map of Babol through Boulanger & Idriss [46] method

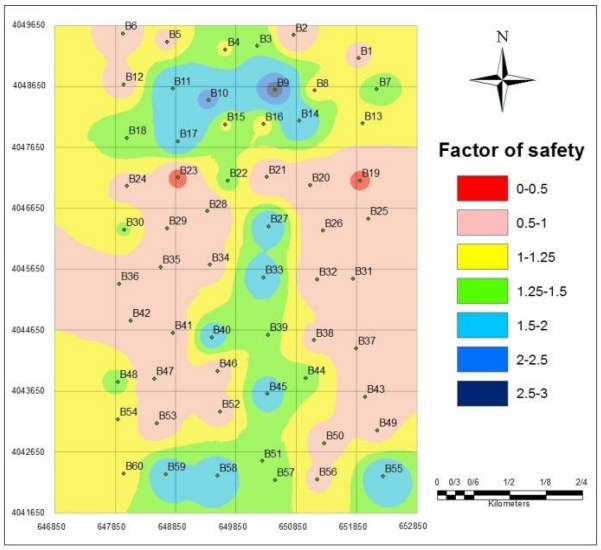

Fig. 10 - Liquefaction map of Babol through Andrus & Stokoe [47] method

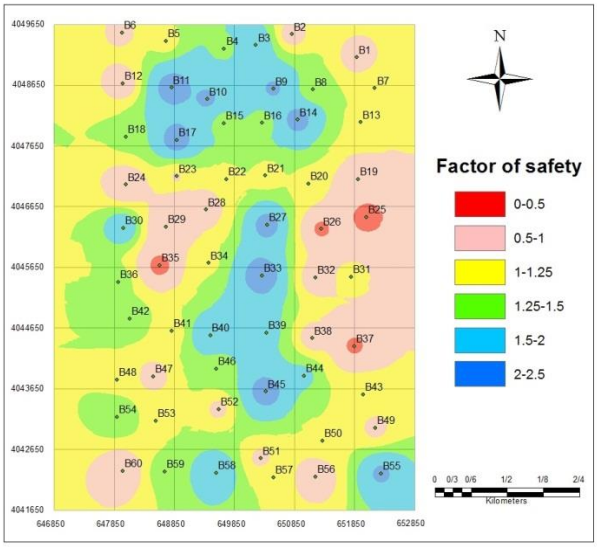

Fig. 11 - Liquefaction map of Babol through Moss et al. [48] method

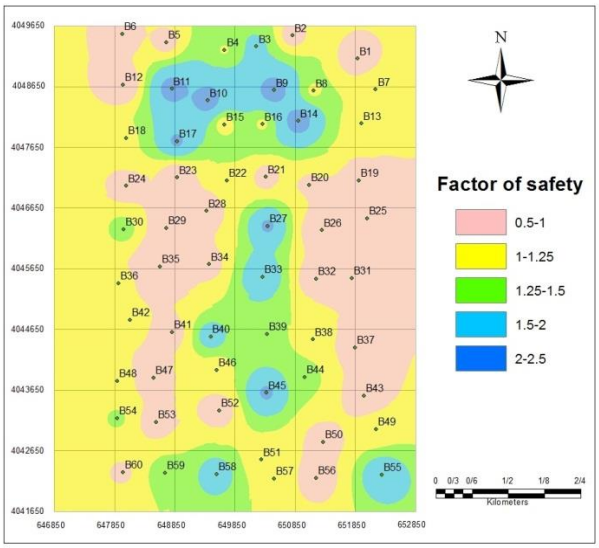

Fig. 12 - The average results found for liquefaction map of Babol

Fig. 13 depicts the liquefaction map of Babol suggested by Rezaei & Choobbasti [44]. In their study, Babol soil liquefaction potential was evaluated using artificial neural networks (ANN). The input–output data pairs utilized in their research consisted of four input variables, including corrected SPT blow count, total stress, effective stress and soil type and one output factor of safety. After training process, the capability of their proposed ANN model for the liquefaction prediction was assessed. Then, the network performance was tested through remaining data pairs. According to their findings, the trained network can successfully model and predict the outputs and can be employed in the prediction of liquefaction potential.

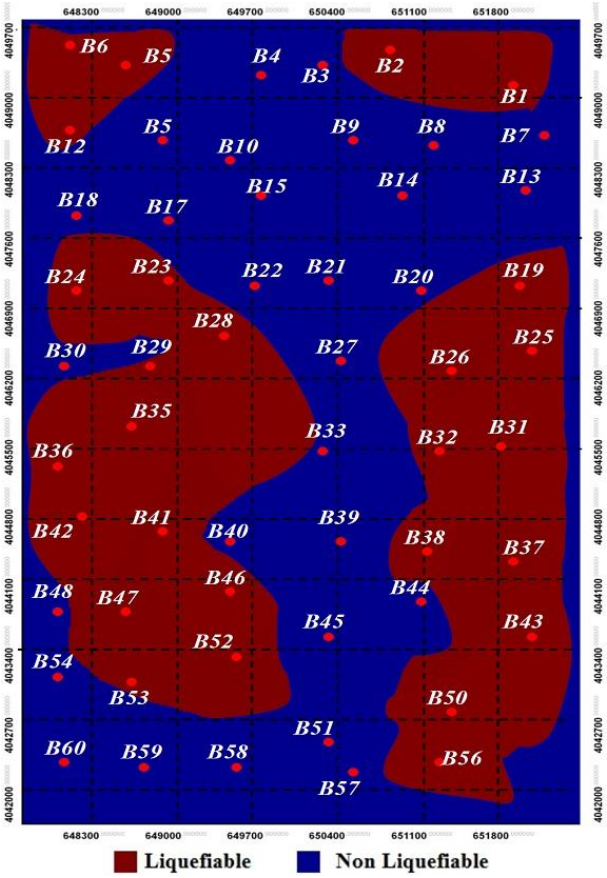

Fig. 13 - Liquefaction map of Babol using ANN [44]

Liquefaction map of Babol through Andrus & Stokoe [47] method (Fig. 10) and the average results (Fig. 12) have good compatibility with Fig. 13. These results show that although the CPT and SPT are the two most widely utilized indices for estimating the liquefaction properties of soils [55], [56], the standard penetration number (N) and cone tip resistance (q_c) are not evaluated precisely and the test apparatus may be in error. In addition, due to the variation of the recorded SPT N-value and CPT resistance, factor of safety against liquefaction may lead to an over or under estimation compare to each other. Some researchers such as Hoque et al. [57] recommended the employment of high-quality tests for an accurate and reliable estimation of liquefaction when both methods of SPT and CPT are utilized in combinations. Therefore, the measurement of shear wave velocity (V_s), as a significant soil characteristic in earthquake site response [58], is essential for evaluation of liquefaction potential. The V_s-based approaches are believed to be useful methods for estimation of liquefaction because V_s can represent the dynamic characteristics of soil acceptably and also soil liquefaction is ascribed to the soil dynamic properties.

5. Conclusions

The utilization of various liquefaction estimation procedures provides a useful tool for assessing soil liquefaction potential. The SPT, CPT and Vs are the tests that are most commonly utilized for this purpose. For liquefaction estimation, each of the mentioned tests (SPT, CPT and Vs) has its own benefits and disadvantages. In the present research, based on the geotechnical data of 60 boreholes, liquefaction potential of Babol soil was evaluated by three methods including Boulanger & Idriss [46], Andrus & Stokoe [47] and Moss et al. [48] methods. Then, the obtained liquefaction maps were compared. Finally, by averaging factor of safety values, a comprehensive liquefaction map was provided for Babol city. The results depicted that the factor of safety of less than one (liquefaction) takes place in 45% of the Babol city.

The findings of the present study were in strong agreement with the results of previous investigations. Since many factors such as soil type, fines content, type of tests and their precision can affect liquefaction, it would be much safer to conduct different field tests for the same place and then compare the results to assess the potential of liquefaction. Therefore, it can be concluded that using only one method for liquefaction evaluation is not enough. The application of different approaches decreases error probability and leads to a more accurate evaluation of the liquefaction potential.

Acknowledgement

The authors would like to acknowledge the Department of Civil Engineering, Babol Noshirvani University of Technology, and Department of Engineering, Shargh-e Golestan Institute of Higher Education, Iran.

References

[1] Rezaei, S., Shooshpasha, I. & Rezaei, H. (2019). Reconstruction of landslide model from ERT, geotechnical and field data, Nargeschal landslide, Iran. Bulletin of Engineering Geology and the Environment, 78, 3223-3237
[2] Rezaei, S., Shooshpasha, I. & Rezaei, H. (2020). Evaluation of landslides using ambient noise measurements (case study: Nargeschal landslide). International Journal of Geotechnical Engineering, 14(4), 409-419
[3] Wu, K., Chen, N., Hu, G., Wang, T., Zhang, Y. & Marcelo, S. (2021). New insights into the failure mechanism and dynamic process of the Boli landslide, China. Bulletin of Engineering Geology and the Environment, 80, 2131-2148
[4] Othman, B.A. & Marto, A. (2019). A liquefaction resistance of sand-fine mixtures: short review with current research on factors influencing liquefaction resistance. International Journal of Integrated Engineering, 11(7), 20-30
[5] Choobbasti, A.J., Rezaei, S. & Farrokhzad, F. (2013). Evaluation of site response characteristics using microtremors. Gradevinar, 65(8), 731–741
[6] Xiu, X., Wang, S., Ji, Y., Wang, F. & Ren, F. (2020). Experimental investigation on liquefaction and post-liquefaction deformation of stratified saturated sand under cyclic loading. Bulletin of Engineering Geology and the Environment, 79, 2313-2324
[7] Shooshpasha, I., Hasanzadeh, A. & Taghavi, A. (2013). Prediction of the axial bearing capacity of piles by SPT-based and numerical design methods. International Journal of GEOMATE, 4(8), 560–564
[8] Shooshpasha, I., Kharun, M. & Hasanzadeh, A. (2017). Evaluation of end bearing capacity of drilled shafts in sand by numerical and SPT-based methods. Journal of Fundamental and Applied Sciences, 9(7S), 282-295
[9] Zhang, J., Xiao, S., Huang, H. & Zhou, J. (2020). Calibrating a standard penetration test based method for region-specific liquefaction potential assessment. Bulletin of Engineering Geology and the Environment, 79, 5185-5204
[10] Kishida, H. (1966). Damage to reinforced concrete buildings in Niigata city with special reference to foundation engineering. Soils and Foundations, 6(1), 71–86
[11] Ohsaki, Y. (1966). Niigata earthquake, 1964, building damage and soil condition. Soils and Foundations, 6(2), 14–37
[12] Tunusluoglu, M.C. & Karaca, O. (2018). Liquefaction severity mapping based on SPT data: a case study in Canakkale city (NW Turkey). Environmental Earth Sciences, 77, 1-29. https://doi.org/10.1007/s12665-018-7597-x
[13] Cetin, K.O., Seed, R.B., Kiureghian, A.D., Tokimatsu, K., Harder, Jr. L.F., Kayen, R.E. & Moss, R.E.S. (2004). Standard penetration test-based probabilistic and deterministic assessment of seismic soil liquefaction potential. Journal of Geotechnical and Geoenvironmental Engineering, ASCE, 130(12), 1314-1340
[14] Cetin, K.O., Seed, R.B., Kayen, R.E., Moss, R.E.S., Bilge, H.T., Ilgac, M. & Chowdhury, K. (2018). The use of the SPT-based seismic soil liquefaction triggering evaluation methodology in engineering hazard assessments. MethodsX, 5, 1556-1575
[15] Seed, H.B., Tokimatsu, K., Harder, L. & Chung, R. (1985). Influence of SPT procedures in soil liquefaction resistance evaluations. Journal of Geotechnical Engineering, ASCE, 111(12), 1425-1445
[16] Kumar, V. & Rawat, A. (2017). Soil liquefaction and its evaluation based on SPT by soft-computing techniques. MATTER: International Journal of Science and Technology, 3(2), 316-327
[17] Goharzay, M., Noorzad, A., Ardakani, A.M. & Jalal, M. (2017). A worldwide SPT-based soil liquefaction triggering analysis utilizing gene expression programming and Bayesian probabilistic method. Journal of Rock Mechanics and Geotechnical Engineering, 9(4), 683-693
[18] Muduli, P.K. & Das, S.K. (2015). Model uncertainty of SPT-based method for evaluation of seismic soil liquefaction potential using multi-gene genetic programming. Soils and Foundations, 55(2), 258-275
[19] Cabalar, A.F., Canbolat, A., Akbulut, N., Tercan, S.H. & Isik, H. (2019). Soil liquefaction potential in Kahramanmaras, Turkey. Geomatics, Natural Hazards and Risk, 10(1), 1822-1838, https://doi.org/10.1080/19475705.2019.1629106
[20] Zhou, S. (1980). Evaluation of the liquefaction of sand by static cone penetration test. Proceedings of 7th World Conference on Earthquake Engineering, Istanbul, Turkey
[21] Lees, J.J., Ballagh, R.H., Orense, R.P. & Ballegooy, S.V. (2015). CPT-based analysis of liquefaction and re-liquefaction following the Canterbury earthquake sequence. Soil Dynamics and Earthquake Engineering, 79, 304-314
[22] Chen, T. & Yuan, X. (2014). Examination of CPT-based liquefaction evaluation methods for New Zealand earthquake. Applied Mechanics and Materials, 477-478, 1105-1108

[23] Mola-Abasi, H., Kordtabar, B. & Kordnaeij, A. (2018). Liquefaction prediction using CPT data by triangular chart identification. International Journal of Geotechnical Engineering, 12(2), 377-382
[24] Chen, Q., Wang, C. & Juang, C.H. (2016). CPT-based evaluation of liquefaction potential accounting for soil spatial variability at multiple scales. Journal of Geotechnical and Geoenvironmental Engineering, 142(2), https://doi.org/10.1061/(ASCE)GT.1943-5606.0001402
[25] Rezania, M., Javadi, A.A. & Giustolisi, O. (2010). Evaluation of liquefaction potential based on CPT results using evolutionary polynomial regression. Computers and Geotechnics, 37(1-2), 82-92
[26] Vivek, B. & Raychowdhury, P. (2014). Probabilistic and spatial liquefaction analysis using CPT data: a case study for Alameda County site. Natural Hazards, 71, 1715–1732
[27] Setiawan, B. & Jaksa, M. (2018). Liquefaction assessment using the CPT and accounting for soil aging. Aceh International Journal of Science and Technology, 7(3), 162-168
[28] Robertson, P.K. (2010). Evaluation of flow liquefaction and liquefied strength using the Cone Penetration Test. Journal of Geotechnical and Geoenvironmental Engineering, ASCE, 136(6), 842-853
[29] Rezaei, S., Shooshpasha, I. & Rezaei, H. (2020). Evaluation of ground dynamic characteristics using ambient noise measurements in a landslide area. Bulletin of Engineering Geology and the Environment, 79, 1749-1763
[30] Rezaei, S. & Choobbasti, A.J. (2020). Site response evaluation through measuring the ambient noise (case study: Babol city). Innovative Infrastructure Solutions, 5, https://doi.org/10.1007/s41062-020-0272-6
[31] Rezaei, S., Shooshpasha, I. & Rezaei, H. (2018). Empirical correlation between geotechnical and geophysical parameters in a landslide zone (case study: Nargeschal landslide). Earth Sciences Research Journal, 22(3), 195-204
[32] Ahmadi, M.M. & Akbari Paydar, N. (2014). Requirements for soil-specific correlation between shear wave velocity and liquefaction resistance of sands. Soil Dynamics and Earthquake Engineering, 57, 152–163
[33] Askari, F., Dabiri, R., Shafiee, A. & Jafari, M.K. (2011). Liquefaction resistance of sand-silt mixtures using laboratory based shear wave velocity. International Journal of Civil Engineering, 9(2), 135-144
[34] Baxter, C., Bradshaw, A., Green, R. & Wang, J. (2008). Correlation between cyclic resistance and shear-wave velocity for providence silts. Journal of Geotechnical and Geoenvironmental Engineering, ASCE, 134(1), 37–46
[35] Amoly, R.S., Ishihara, K. & Bilsel, H. (2016). The relation between liquefaction resistance and shear wave velocity for new and old deposits. Soils and Foundations, 56(3), 506-519
[36] Kayen, R., Moss, R.E.S., Thompson, E.M., Seed, R.B., Cetin, K.O., Der Kiureghian, A., Tanaka, Y. & Tokimatsu, K. (2013). Shear-wave velocity–based probabilistic and deterministic assessment of seismic soil liquefaction potential. Journal of Geotechnical and Geoenvironmental Engineering, ASCE, 139(3), 407-419
[37] Asadi, M.B., Asadi, M.S., Orense, R.P. & Pender, M.J. (2018). Shear wave velocity-based assessment of liquefaction resistance of natural pumiceous sands. Géotechnique Letters, 8(4), 262-267
[38] Rahmanian, S. & Rezaie, F. (2017). Evaluation of liquefaction potential of soil using the shear wave velocity in Tehran, Iran. Geosciences Journal, 21, 81–92
[39] Guoxing, C., Mengyun, K., Khoshnevisan, S., Weiyun, C. & Xiaojun, L. (2019). Calibration of Vs-based empirical models for assessing soil liquefaction potential using expanded database. Bulletin of Engineering Geology and the Environment, 78, 945–957
[40] Xu, X.M., Ling, D.S., Cheng, Y.P. & Chen, Y.M. (2015). Correlation between liquefaction resistance and shear wave velocity of granular soils: a micromechanical perspective. Géotechnique, 65(5), 337-348
[41] Oka, L.G., Dewoolkar, M. & Olson, S.M. (2018). Comparing laboratory-based liquefaction resistance of a sand with non-plastic fines with shear wave velocity-based field case histories. Soil Dynamics and Earthquake Engineering, 113,162-173
[42] Kamel, F. & Badreddine, S. (2020). Liquefaction analysis using shear wave velocity. Civil Engineering Journal, 6(10), 1944-1955
[43] Farrokhzad, F., Choobbasti, A.J. & Barari, A. (2012). Liquefaction microzonation of Babol city using artificial neural network. Journal of King Saud University, 24(1), 89-100
[44] Rezaei, S. & Choobbasti, A.J. (2014). Liquefaction assessment using microtremor measurement, conventional method and artificial neural network (case study: Babol, Iran). Frontiers of Structural and Civil Engineering, 8, 292-307
[45] Taghavinezhad, M., Choobbasti, A.J. & Farrokhzad, F. (2019). Effect of liquefaction on nonlinear seismic response in layered soils: a case study of Babol, north of Iran. European Journal of Environmental and Civil Engineering, https://doi.org/10.1080/19648189.2019.1623081
[46] Boulanger, R.W. & Idriss, I.M. (2012). Probabilistic SPT-based liquefaction triggering procedure. Journal of Geotechnical and Geoenvironmental Engineering, ASCE, 138(10), 1185–1195
[47] Andrus, R.D. & Stokoe, K.H. (2000). Liquefaction resistance of soils from shear-wave velocity. Journal of Geotechnical and Geoenvironmental Engineering, ASCE, 126(11), 1015-1025
[48] Moss, R.E.S., Seed, R.B., Kayen, R.E., Stewart, J.P., Der Kiureghian, A. & Cetin, K.O. (2006). CPT-based probabilistic and deterministic assessment of in situ seismic soil liquefaction potential. Journal of Geotechnical and Geoenvironmental Engineering, ASCE, 132(8), 1032-1051

[49] Choobbasti, A.J., Rezaei, S., Farrokhzad, F. & Haidarzadeh Azar, P. (2014). Evaluation of site response characteristic using nonlinear method (case study: Babol, Iran). Frontiers of Structural and Civil Engineering, 8, 69-82
[50] Rezaei, S. & Choobbasti, A.J. (2018). Evaluation of local site effect from microtremor measurements in Babol City, Iran. Journal of Seismology, 22, 471-486
[51] Ahmadi, G., Keshtkar, R., Mavizchi, M. & Vetr, M.G. (2014). Using seismic hazard assessment to study dynamic behavior of Gonbad-e Kāvus tower (the tallest brick tower in the world). International Journal of Advanced Structural Engineering (IJASE), 6(4), 133-148
[52] Seed, H.B. & Idriss, I.M. (1971). Simplified procedure for evaluating soil liquefaction potential. Journal of Soil Mechanics and Foundations Division, ASCE, 97(9), 1249-1273
[53] Building and Housing Research Center. (2015). Standard 2800, Iranian Code of Practice for Seismic Resistant Design of Building (4th ed)
[54] Hakam, A., Warzuqni, S., Adji, B.M., Junaidi, Muharani, I.F. & Mardhatillah. (2020). CPT -D_R-D_{50} correlations of sands for liquefaction potential analysis. E3S Web of Conferences, 156, 1-6
[55] Stacul, S., Magalotti, A., Baglione, M., Meisina, C. & Lo Presti, D. (2020). Implementation and use of a mechanical cone penetration test database for liquefaction hazard assessment of the coastal area of the Tuscany region. Geosciences, 10(4), 1-25
[56] Du, G., Gao, C., Liu, S., Guo, Q. & Luo, T. (2019). Evaluation method for the liquefaction potential using the standard penetration test value based on the CPTU soil behavior type index. Advances in Civil Engineering, 2019, 1-8
[57] Hoque, M.M., Ansary, M. & Siddique, A. (2017). Evaluation of liquefaction potential from SPT and CPT: a comparative analysis. Proceedings of the 19th International Conference on Soil Mechanics and Geotechnical Engineering, Seoul, South Korea
[58] Liew, M., Xiao, M., Liu, S. & Rudenko, D. (2020). In situ seismic investigations for evaluating geotechnical properties and liquefaction potential of fine coal tailings. Journal of Geotechnical and Geoenvironmental Engineering, ASCE, 146(5), 04020014